



ELSEVIER

journal homepage: [www.elsevier.com/locate/jmatprotec](http://www.elsevier.com/locate/jmatprotec)

# Characterization of spray lubricants for the high pressure die casting processes

Adrian S. Sabau\*, Ralph B. Dinwiddie

Materials Science and Technology Division, Oak Ridge National Laboratory, Bldg. 4508,  
MS 6083, Oak Ridge, TN 37831-6083, United States

## ARTICLE INFO

### Article history:

Received 9 January 2007

Received in revised form

12 April 2007

Accepted 10 May 2007

### Keywords:

Die casting

Die lubrication

Heat flux measurement

Spray cooling

Heat transfer

Infrared visualization

## ABSTRACT

During the high pressure die casting process, lubricants are sprayed in order to cool the dies and facilitate the ejection of the casting. The cooling effects of the die lubricant were investigated using thermogravimetric analysis (TGA), heat flux sensors (HFS), and infrared imaging. The evolution of the heat flux and pictures taken using a high-speed infrared camera revealed that lubricant application was a transient process. The short time response of the HFS allows the monitoring and data acquisition of the surface temperature and heat flux without additional data processing. A similar set of experiments was performed with deionized water in order to assess the lubricant effect. The high heat flux obtained at 300 °C was attributed to the wetting and absorbent properties of the lubricant. Pictures of the spray cone and lubricant flow on the die were also used to explain the heat flux evolution.

© 2007 Published by Elsevier B.V.

## 1. Introduction

During the die casting process, the dies are sprayed with a lubricant, dies are closed, and liquid metal is injected into the die cavity under high pressures. Net shape parts are produced after subsequent metal solidification and cooling, dies are opened, and parts are ejected. Lubricants facilitate the ejection of the finished product, reduce the soldering effects (Fraser and Jahedi, 1997), and cool the dies (Piskoti, 2003). The lubricant film thickness on the die surface was used to quantify the lubricant adhesion performance. The lubricant film thickness was usually determined indirectly, using optical or X-ray techniques (Fraser and Jahedi, 1997) or die temperature (Piskoti, 2003). Channels are drilled into the dies for heating or cooling in order to maintain temperature levels that will yield progressive solidification and uniform cooling of the parts. In

order to minimize casting defects, the metal delivery and heating/cooling systems are designed based on the analysis of heat transfer and solidification phenomena. One of the parameters required for the die design is the amount of heat removed during lubricant application. Data on heat transfer coefficients or heat flux evolution during lubricant application are used to characterize the heat removal capability of lubricants and perform numerical simulations of the die casting process (Liu et al., 2000).

Spray cooling was mainly studied for other applications than the die casting process. There is significant effort on the study of spray impingement for power electronics using water and refrigerants, and steel industry using water and oils (Stewart et al., 1995). Few predictive models for heat transfer exist other than those for critical heat flux (CHF) (Pautsch and Shedd, 2005). A CHF correlation that accounts for volumetric

\* Corresponding author. Tel.: +1 865 241 5145; fax: +1 865 574 4357.

E-mail address: [sabaua@ornl.gov](mailto:sabaua@ornl.gov) (A.S. Sabau).

0924-0136/\$ – see front matter © 2007 Published by Elsevier B.V.

doi:10.1016/j.jmatprotec.2007.05.021

### Nomenclature

$df/dt$	weight fraction rate (1/s)
DTA	differential thermal analysis
DTG	first derivative thermogravimetry, i.e., $df/dt$
$f$	weight fraction
$h$	heat transfer coefficient ( $W/m^2 K$ )
HAZ	heat affected zone
HFS	heat flux sensor
$q''$	heat flux ( $W/m^2$ )
$T_A$	ambient temperature ( $25^\circ C$ )
$T_S$	plate surface temperature ( $^\circ C$ )
TGA	thermogravimetric analysis

flow rate, fluid properties, spray angle, droplet diameter, and subcooling was proposed by Mudawar and Estes (Mudawar and Estes, 1996). For low superheat, Hsieh et al. (Hsieh et al., 2004a) presented correlations for heat flux removed as a function of dimensionless parameters such as droplet Weber number and liquid Jacob number. Although this information would be useful for the formulation of new lubricants, it is difficult, if not impossible, to use correlations on boiling, droplet or water sprays developed for other processes. For example, boiling in droplets deposited on a hot surface differs from that observed in a pool boiling, since heat transfer relies on the contact area between the droplets and surface (Cui et al., 2003). The correlations obtained in the spray impingement studies are not applicable to the lubricant application process since there are significant differences between these processes. These differences include:

- Different superheat: in the die casting process, the superheat varies from  $150$  to  $400^\circ C$ , while for power electronics and steel quenching is approximately less than  $150$  and larger than  $1100^\circ C$ , respectively;
- different surface materials;
- different flow rates;
- transient versus uniform: most of boiling studies are for uniform state processes while the die lubrication is very transient, lasting from  $0.2$  to several seconds.

In the steady-state boiling three distinct regions exist: forced convection and evaporation, nucleate boiling, and critical heat flux, while in the transient cooling, the film boiling and transition boiling play an important role (Hsieh et al., 2004b). Gonzalez and Black (Gonzalez and Black, 1997) found that the interaction between spray and buoyant jet issued from a heated surface would reduce the droplet velocity.

The first principle approach, which was used to investigate spray cooling for other industries, is useful to investigate the fundamental phenomena and assess the effect of numerous parameters, but it would be difficult to implement in a plant environment. Other techniques, such as visualization had been recently used for the study of spray cooling. For low superheats, an array of individually controlled microheaters mounted on a transparent silica substrate was employed (Horacek et al., 2005). The spatial distribution of the heat flux was obtained at constant surface temperature while visual-

ization and measurements of the liquid–solid contact area and the three-phase contact line length were made using an internal reflectance technique (Horacek et al., 2005). For die lubrication, the interaction between powder lubricants and molten alloy was observed with high-speed video system (Kimura et al., 2002). The result of in situ observation revealed that an enhanced insulating ability was due to formation of thin gaseous film between molten alloy and die by vaporized wax.

In most studies on the lubricant application effects, heated plate systems that mimic the die casting dies were employed and temperature data were obtained using thermocouples that were embedded into the plates (Lee et al., 1989; Garrow, 2001). The heat transfer coefficients (or heat fluxes) were obtained using either simple data extrapolation or inverse heat transfer procedures. In some of these studies, the data were recorded at low frequencies, e.g., only two data points per second were taken in Liu et al. (Liu et al., 2000). Due to the thermocouple response time, the temperature data could be very different than the actual temperature. In order to avoid cumbersome analysis of the data, such as performing inverse heat transfer analysis or accounting for the thermocouple response time (Reichelt et al., 2002), a sensor was used by Sabau and Wu (Sabau and Wu, 2007) for the direct measurement of heat flux. In addition to the heat flux data, the sensor provided data on the surface temperature, enabling the computation of the heat transfer coefficient. The temperature distribution of the average heat flux for water spray, which was presented by Sabau and Wu (Sabau and Wu, 2007), was similar that for the well-known pool-boiling curve, validating the use of these sensors for the direct measurement of heat fluxes under conditions specific to the die casting process.

In this study, a complementary effort to the first principle approach was undertaken to characterize the lubricant performance. The lubricant behavior was evaluated using thermogravimetric analysis (TGA), heat flux sensors (HFS), and infrared imaging. The Diluco 135<sup>TM</sup> lubricant, which was supplied by Cross Chemical Company, Inc., was used in this study. This Diluco lubricant was formulated for magnesium castings. Based on the information provided by the manufacturer, this lubricant was formulated with refined oils, natural and synthetic polymers, natural and synthetic waxes, wetting agents and emulsifying agents in order to aid in the mold release process. A dilution ratio of 15:1 for the water:lubricant mixture was recommended by the manufacturer.

In the second section, thermogravimetric analysis differential thermal analysis (DTA) was used to determine lubricant decomposition characteristics since these properties of the lubricant are important for its performance and casting quality. For example, if the lubricant vaporizes fast and at low temperatures, the molten metal would make contact directly with the die material and lubricant would not fulfill its function. On the other hand, if the atmosphere in the die cavity would include significant amounts of volatile decomposition products, there is higher probability of gas entrapped into the molten metal, giving rise to defects that would decrease the casting quality. In the third section, the results for the heat flux and surface temperature, which were measured using a heat flux sensor, were presented. During the experiments, the distance between the spray nozzle and plate was held constant.

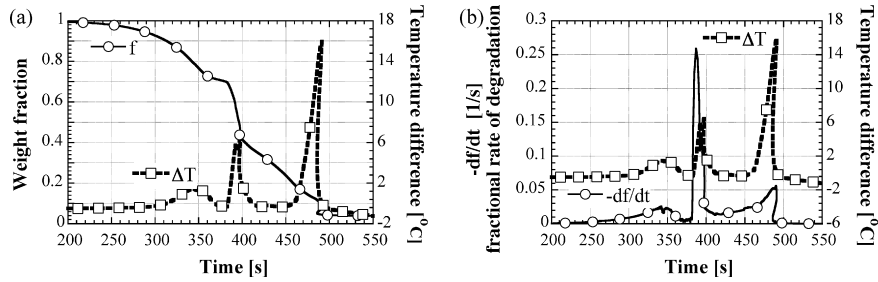


**Fig. 1 – TGA (solid line) and DTA (dotted line) data for Diluco 135™ for a heating rate of 5 °C/min. (b) DTG (dotted line) and DTA (solid line) results for a heating rate of 5 °C/min.**

All the experiments were conducted with the same spray flow parameters (i.e., air pressure, air flow rate, water pressure, water flow rate, and water temperature). Pictures for the lubricant flow patterns were used to explain the distribution of the heat flux at various plate temperatures. In the fourth section, results for the infrared imaging of the spray were presented and discussed. The infrared imaging provided information on the temperature variation within the spray cone. The region of the spray, which had a higher temperature than the ambient temperature, was referred to as heat affected zone (HAZ). Several pictures taken at the initial stages and at large times were shown and discussed. Although the results are presented for the case in which the nozzle was held in the same position for the entire spray application, the HFS and infrared imaging can be used for other spray application techniques, such as pulsing and sweeping. The type of data obtained in this study can be used in the development of new lubricants and the selection of appropriate lubricant application techniques. The HFS and infrared imaging can be used to investigate the cooling effect due to the lubricant application in industrial settings.

## 2. Lubricant decomposition

TA Instruments SDT 2960 module performed both TGA and DTA measurements at the same time. The TGA measurement provided the fraction of volatile components by monitoring the weight change that occurred as a specimen was heated. The DTA data identified the temperature regions and magnitude of critical events during heating. The energy released/absorbed due to chemical reactions or phase changes during the heating process could also be provided by some instruments.

The measurements were performed in an air atmosphere. The samples have been dried out before TGA/DTA measurements have been performed. The TGA/DTA experiments are shown in Figs. 1 and 2 for a heating rate of 5 and 10 °C/min, respectively. Physical changes that involve a change in energy, such as a phase change, without a change in mass were captured in the DTA curve. In order to assess if there were such phenomena, first derivative thermogravimetry (DTG), i.e.,  $-df/dt$ , was obtained. As shown in Fig. 1b, the DTA and DTG indicate the same transition temperatures. Since DTA and DTG show the same transitions, the DTA data was used to describe the degradation of the lubricant. The sample started to volatilize at about 250 °C. The lubricant degraded in three

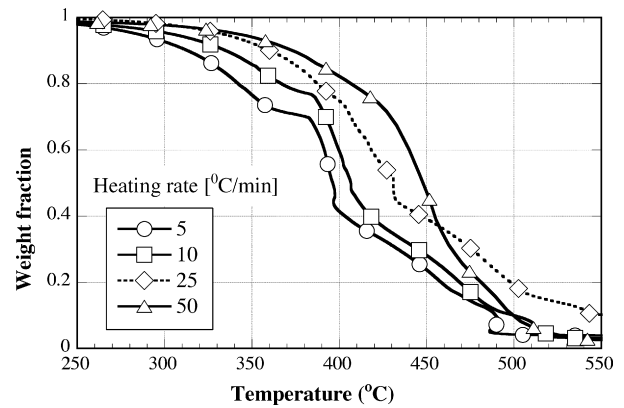


**Fig. 2 – TGA data at different heating rates.**

main stages at temperatures around 345, 390, and 485 °C. In the first and third transitions, the lubricant degraded slowly. In the first and second stages, about 30 and 40–50% of lubricant volatilized. The second transition was the fastest among all three. The data shows that at least 70% of the lubricant was not decomposed below 380 °C, indicating that there should be enough lubricant left on the die before the molten metal is injected into the die.

The lubricant is applied in the die casting process by spraying the diluted lubricant on the die surface. Thus, the lubricant experiences high heating rates during its application on the die and further contact with molten metal. Thus, the kinetics of the degradation events was important for our application. The TGA data was obtained at heating rates of 5, 10, 25, and 50 °C/min. The transition temperatures increase with heating rates. At high heating rates, the TGA curve shows less resolution than those at small heating rates. The results are presented in Fig. 2. This TGA data at different heating rates can be used to determine the kinetic parameters (Kubicek and Lesko, 1979).

## 3. Lubricant application experiments

In order to reproduce conditions similar to those encountered during lubrication of the dies, a heated plate was employed in this study. The test plate was manufactured from H13 steel, which is a common material used to make dies (Fig. 3). The test plate dimensions were 10.2 cm × 12.7 cm × 1.3 cm. The plate

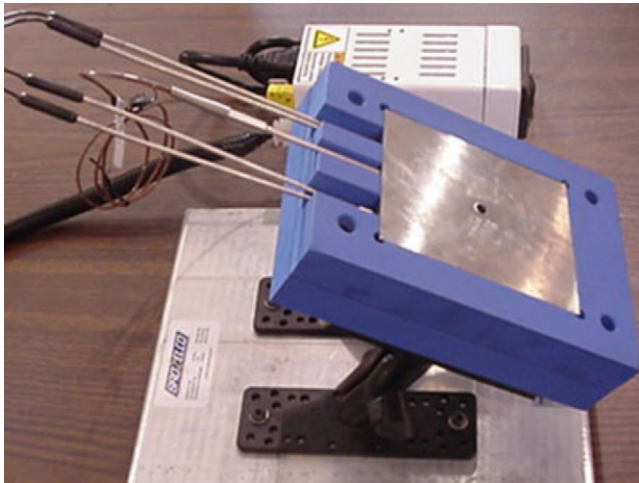


**Fig. 3 – The H13 steel test plate (front) and temperature controller console (back). Dimensions were 10.2 cm × 12.7 cm steel plate and 15.2 cm × 20.3 cm for the insulation with the steel plate.**

was insulated to reduce the heat loss from it and to ensure that heat was mainly conducted to the spray cooled surface (Liu et al., 2000). The edges of the test plate were sealed with silicon to prevent water from penetrating the test plate assembly during spray cooling (Sabau and Wu, 2007; Sabau and Hatfield, 2007). The spray nozzle was placed 190 mm away from the test plate. The nozzle was oriented such that the liquid spray was perpendicular to the center of the plate. The nozzle was held by fixtures to eliminate the heat flux variation due to variability in the nozzle position and orientation. The experiments were conducted at initial plate temperatures of 150, 200, and 300 °C for lubricant and deionized water. The liquid temperature was 25 °C. The liquid and air pressure were each set to 0.446 MPa (50 psi). The test cases were labeled with L# and W# for the lubricant and water experiments, respectively, where # indicate the initial plate temperature. For example, the notation L150 refers to all the runs that were conducted at an initial plate temperature of 150 °C. Different runs, which were performed for each test case, showed that the data acquired had a high degree of reproducibility (Sabau and Hatfield, 2007). The total lubricant spray flow rate through the nozzle was found to be 10.5 cm<sup>3</sup>/s. The liquid mass flow rate on the sensing area was not measured since it was not an engineering variable that can be measured easily during the die lubrication process. Most data on fundamental studies on spray cooling

are reported as heat flux versus surface temperature. In die casting processes, the lubricant application seldom reaches a uniform steady state, as the lubricant is applied for fractions of second or few seconds. Thus, in this paper most of the data is presented as heat flux versus time and surface temperature versus time. The evolution in time of the heat flux and surface temperature is discussed in this section.

### 3.1. Heat flux sensor

An HFM-8E/H heat flux sensor, which was supplied by the Vatel Corporation, was used to acquire data on heat flux and surface temperature. The heat flux sensor was mounted in the center of the test plate. The heat flux sensor was a differential thermopile. Information regarding the heat flux sensor was supplied by the manufacturer and was provided in previous studies (Sabau and Wu, 2007; Sabau and Hatfield, 2007). The heat flux and temperature sensors are thin films deposited by proprietary techniques onto a substrate. The films that make up the HFM are less than 2 μm thick. Due to the thickness of these films, the response time for this heat flux sensor is approximately 6 μs. The sensor thermocouple and differential thermopile was calibrated using NIST traceable equipment. Through calibration, all sensor constants needed to obtain the heat flux (W/m<sup>2</sup>) are provided. This sensor was rated for temperatures up to 700 °C and had a sensitivity of 150 ± 10 μV/W/cm<sup>2</sup>. A data acquisition provided by Dataq Instruments, Inc. was used to obtain data at a sample rate of 60 Hz. The plate surface temperature was considered to be that measured by the thermocouple in the heat flux sensor since the thermocouple is embedded very close to the surface.

### 3.2. Heat flux data

The results for the surface temperature and heat flux were shown in Fig. 4a and b, respectively, for the three cases considered. For the L150 case, it was observed that the plate surface temperature,  $T_s$ , decreased by 25 °C in 8 s. In the first 0.5 s, the temperature dropped to 135 °C and then rose to 140 °C. This zigzag variation was observed for both L150 and L200 cases. For L150 case, the heat flux decreased by a half, to almost 250 kW/m<sup>2</sup>. The results for the L150 and L200 cases are similar in the features, although the maximum heat flux was approximately 300 kW/m<sup>2</sup> higher than that for case L150. From 0.5 to 2 s, the temperature exhibited very small variations, as the heat flux continued to decrease. In the last 5 s of the spray, there was a low degree of superheat, small amount of liquid boiled, and the heat removal was mainly due to the liquid con-

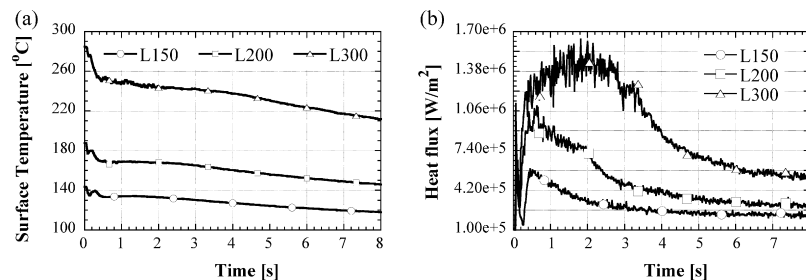


**Fig. 4 – Evolution of: (a) surface temperature and (b) heat flux for cases L150, L200, and L300.**

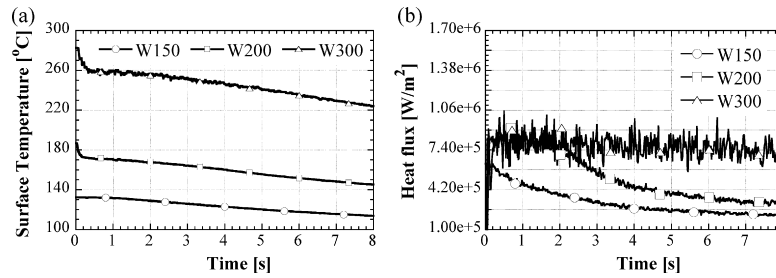


Fig. 5 – Evolution of: (a) surface temperature and (b) heat flux for cases W150, W200, and W300.

vection (Altan et al., 1991). The distribution of the heat flux and surface temperature changed for case L300, i.e., the heat flux stayed relatively constant at its maximum value for a relatively larger time. The initial constant heat flux stage lasted approximately 3 s for L300 case. Also, the zigzag variation of  $T_s$ , which was a characteristic of L150 and L200, had not been observed for L300. Instead,  $T_s$  exhibited a sharp and linear decrease in the first 0.5 s. Numerical simulation results for the evolution of surface temperature in the initial stage showed that the sudden temperature drop was due to high cooling fluxes (Sabau and Wu, 2007).

A similar set of experiments was performed with deionized water in order to assess the lubricant effect. The surface temperature results did not show the zigzag variation at 150 and 200 °C and are close to those for the lubricant (Figs. 4a and 5a). The heat flux results at 150 and 200 °C for both the lubricant and water (Figs. 4b and 5b). The heat flux results for the W300 and L300 cases are very different. While the heat flux for L300 case showed values larger than 1.38 MW/m<sup>2</sup> from 0.8 to 2.8 s, the heat flux for W300 case was almost constant at 0.8 MW/m<sup>2</sup>, which was approximately half of the maximum value for the L300 case. Thus, the highest heat flux for the L300 was due to the lubricant effects. The higher heat flux for the L300 could not be attributed to the phase changes in the lubricant since only a minor fraction of the lubricant was volatilized at 300 °C (Fig. 1a). In addition, the spray cooling was primarily due to the boiling of water since the lubricant content was very small. Instead, the high heat flux for the L300 case was likely to be due to the water absorptivity into the lubricant and wetting of the water-lubricant mixture (Piskoti, 2003). It was known that die lubricants affect the cooling process by providing a substrate capable of absorbing water and holding it close

to the hot surface of the die (Piskoti, 2003). This important mechanism does not occur for pure water, further precluding the use of water spray cooling correlations for the die casting process.

In order to gain insight into the differences between the L200 and L300, the patterns for the spray cone and lubricant flow on the die were investigated. Pictures, which were taken for L200 and L300 cases, were shown in Fig. 6a and b, respectively. The following differences can be seen between these two cases:

- Lubricant was spread over a larger area for L200 than for L300;
- towards the edge of the spread area, the lubricant fingers were larger for L200 than for L300;
- lubricant fingers were thicker for the L200 than for L300;
- spray cone was continuous from the nozzle to the plate for L200, while it was shaped as mushroom for L300.

The mushroom shape for the L300 spray cone was due to the convection of the vapor away from the plate. The higher rate of vaporization for L300 increased the convection of the vapor, which pushes away the lubricant droplets, hindering droplet impingement on the plate surface (Gonzalez and Black, 1997). This behavior was transient. Initially, the vapor layer was not established, all the droplets impacted the surface and vaporized upon contact with the heated surface, resulted in the highest heat flux. As the hot vapor layer was built near the plate surface, droplets partially vaporized before reaching the plate. Also, the droplets on outer surface of the spray cone were decelerated and deviated on paths toward the outer surface by the vapor that flowed away from the center

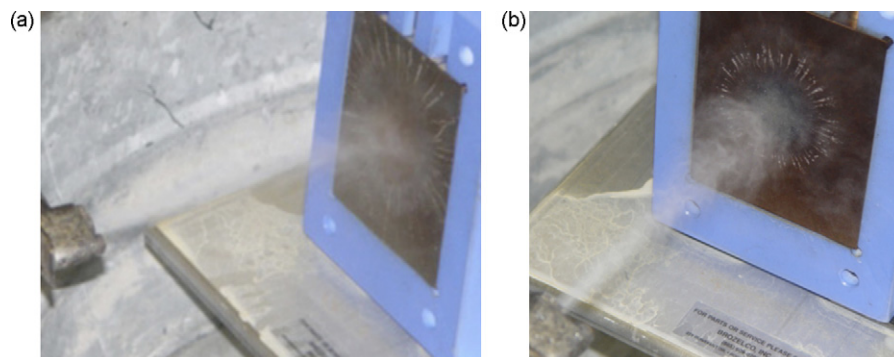


Fig. 6 – Pictures showing liquid streams on the plate for cases: (a) L200 and (b) L300. Water vapors preclude an effective cooling at longer times.

region. These vaporization effects combined with the decrease in surface temperature yield a decrease in the heat flux.

#### 4. Infrared visualization

In order to gain insight on the spray mechanisms, the temperature distribution of the spray cone was monitored using high-speed infrared camera. Images were acquired using the Amber Radiance-HS Midwave IR camera, with a  $256 \times 256$  InSb focal plane array detector that is sensitive to infrared wavelengths from 3000 to 5000 nm. This camera operates in a snapshot mode where all pixels are sampled at the same time. Snapshot mode is useful in reducing blurring and distortions when imaging fast moving targets or scenes where temperature may be changing rapidly. The camera was equipped with a 50 mm germanium lens. The integration time (exposure time) was set to 1.0 ms. A total of 700 images were acquired at 140 Hz for each experiment. Each set of 700 images is referred to as a sequence and can be thought of as a short movie. No filters were required when the plate surface was set to  $150^\circ\text{C}$ . However, two filters were used in series when the plate temperature was set to  $300^\circ\text{C}$ . The filters were standard photographic 80A and cross polarizer filters mounted on the front of the IR lens. In the infrared region these filters basically act as low cost neutral density filters, reducing the overall radiance from the scene. In order to eliminate background clutter, the first image prior to the spray becoming visible was subtracted from the entire sequence. This insures that only the spray cone is visible in the infrared images. Time was set to zero when the spray first hits the plate. The image sequences were colorized, using a consistent color pallet, in order to clearly identify the temperature distribution within the spray cone. This color pallet or color map was set with an IR signal of 0 bit-count being represented by black and the IR signal of 2228 bit-count represented by yellow. Intermediate IR signals were represented by magenta, blue, cyan, green, red, and orange, listed in order on increasing intensity. The IR signal is a relative unitless number which is proportional to the temperature and emissivity of the object being imaged. Other factors that can affect the magnitude of the IR signal (i.e., distance, lens, filters, atmosphere, integration time, background temperature, etc.) were maintained constant, with the exception of filters as discussed above. Changing the filters between the L150 and L300 cases means that, for example, the green region of the L150 case is not the same temperature as the green region of the L300 case. However, when comparing all of the images within the L300 case, all regions represented by a particular color are of the same temperature range. Individual images were selected from each sequence for comparison. These comparison images were acquired at time = 0.021, 0.057, 0.064, 0.086, 1.86, and 3.8 s.

##### 4.1. Infrared imaging results

The results obtained by the infrared camera were shown in Figs. 7 and 8 for cases L150 and L300, respectively. The infrared imaging provided information on the relative temperature variation within the spray cone. This spray cone is referred to in the remainder of the paper as heat affected zone. By elimi-

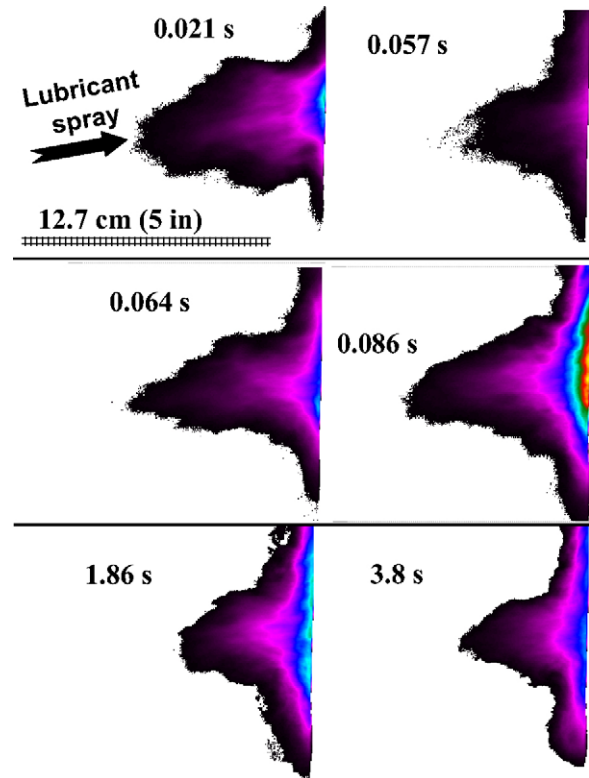
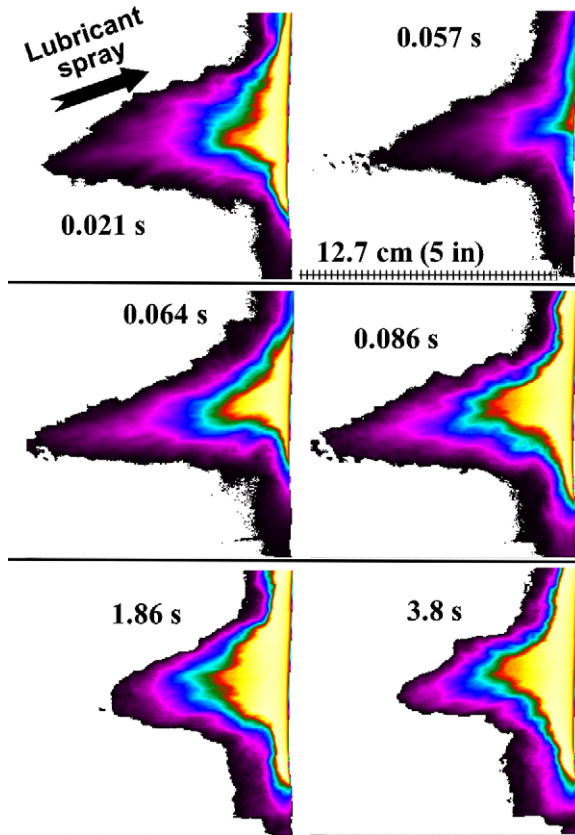


Fig. 7 – Infrared pictures showing the temperature profile in front of the plate for case L150.

nating the pixels with the lowest signal, the air and the spray region that had that lowest temperature were eliminated. The time at which the pictures were taken were shown on each frame. HAZ were inclined since the spray direction was slightly inclined.

For L150 case, the largest HAZ was recorded at 21 ms. The appearance of the largest HAZ at the initial times was consistent to the droplet movement and the convection of the vapors away from the hot plate. Initially, the plate surface had the highest temperature, the vapor blanket would not be established, the droplets would have a higher normal momentum and would get closer to the hot surface, the droplets would vaporize more effective, and the remaining droplets would bounce back with a higher velocity. Droplet bouncing and multiple droplet impact with the hot surface are expected, as showed by the droplet paths in a conical spray (Issa, 2003). For water sprays, a numerical method was presented by Issa (Issa, 2003) that incorporated models for droplet spreading, droplet evaporation near the surface, pressure effect on the latent heat of vaporization, and multiple impact of the droplet. At 57 ms, the HAZ had a lower height near the plate center, but increased its height more uniformly on the plate surface, as compared to those at 21 ms frame. At 64 and 86 ms, the HAZ had a shape similar to that at 21 ms. At large times, the HAZ decreased in size as evidenced by the frames taken at 1.86 and 3.8 s. This evolution of the HAZ can be explained by considering the data on the surface temperature, data on heat flux, and effect of the vapor blanket that was established near the hot surface. As the spray continued, the surface temperature decreased, the



**Fig. 8 – Infrared pictures showing the temperature profile in front of the plate for case L300.**

water vapor slowed the incoming spray droplets, less heat was removed from the surface, and less vaporization took place.

For L300 case, HAZ evolution was similar to that for the L150 case. For the L300 case, there was more detail available as the color map was fully used, and the region of high temperature was fully seen near the hot surface. At 57 ms, it was noted that the maximum temperature in the HAZ was lower than that of the hot plate temperature. Although the HAZ had decreased in size, the HAZ of maximum temperature had stayed the same from 64 ms till 3.8 s. Overall, HAZ was larger for the L300 than for the L150 case. This indicated that a large amount of vapor and droplets with high temperature were present in the L300 case. Thus, it has been demonstrated that infrared imaging can be used to determine the relative temperature variation within the spray cone.

## 5. Conclusion

The cooling effects of the die lubricant were investigated using thermogravimetric analysis, heat flux sensors, and infrared imaging. The TGA data showed that the lubricant started to volatilize at about 250°C and that it degraded in three main stages at temperatures around 345, 390, and 485°C. The evolution of the heat flux and pictures taken using a high-speed infrared camera revealed that lubricant application was a transient process. The short time response of the HFS allows the monitoring and data acquisition of the surface temper-

ature and heat flux without additional data processing. A similar set of experiments was performed with deionized water in order to assess the lubricant effect. It was shown that for diluted lubricant sprays, the measured heat fluxes were different than those for deionized water. The high heat flux obtained at 300°C was attributed to the wetting and absorbent properties of the lubricant. Pictures of the spray cone and lubricant flow on the die were also used to explain the heat flux evolution. Infrared imaging can be used to determine the relative temperature variation within the spray cone.

## Acknowledgments

This work was performed under a Cooperative Research and Development Agreement (CRADA) with the United States Advanced Materials Partnership (USAMP), United States Council for Automotive Research (USCAR) for the project on Structural Cast Magnesium Development. This research was sponsored by the U.S. Department of Energy, Assistant Secretary for Energy Efficiency and Renewable Energy, Office of Transportation Technologies, Lightweight Vehicle Materials Program, under contract DE-AC05-00OR22725 with UT-Battelle, LLC. The authors acknowledge that this research was supported in whole by Department of Energy Cooperative Agreement No. DE-FC05-02OR22910. Such support does not constitute an endorsement by the Department of Energy of the views expressed herein.

## REFERENCES

- Altan, T., Bishop, S.A., Miller, R.A., Chu, Y.L., 1991. A preliminary investigation on the cooling and lubrication of die casting die by spraying. In: NADCA, Detroit-T91-115, pp. 355–361.
- Cui, Q., Chandra, S., McCahan, S., 2003. The effect of dissolving salts in water spray used for quenching a hot surface. Part 1: Boiling of single droplets. *ASME J. Heat Transfer* 125, 326–332.
- Fraser, D.T., Jahedi, M., June 1997. Proceedings of ADCA, Die Casting and Toolmaking Technology Conference, Melbourne. Die Lubrication in High Pressure Die Casting.
- Garrow, D.M., 2001. Characterization of die casting die lubricants. In: MSE 695 Presentation, Ohio State University.
- Gonzalez, J.E., Black, W.Z., 1997. Study of droplet sprays prior to impact on a heater horizontal surface. *ASME J. Heat Transfer* 119, 279–287.
- Horacek, B., Kiger, K.T., Kim, J., 2005. Single nozzle spray cooling heat transfer mechanisms. *Int. J. Heat Mass Transfer* 48, 1425–1438.
- Hsieh, S.S., Fan, T.C., Tsai, H.H., 2004a. Spray cooling characteristics of water and R-134a. Part 1: Nucleate boiling. *Int. J. Heat Mass Transfer* 47, 5703–5712.
- Hsieh, S.S., Fan, T.C., Tsai, H.H., 2004b. Spray cooling characteristics of water and R-134a. Part II: Transient cooling. *Int. J. Heat Mass Transfer* 47, 5713–5724.
- Issa, R.J., Numerical modeling of the dynamics and heat transfer of impacting sprays for a wide range of pressures, Ph.D. Thesis, University of Pittsburgh, Pittsburgh, PA, 2003.
- Kimura, R., Yoshida, M., Sasaki, G., Pan, J., Fukunaga, H., 2002. Characterization of heat insulating and lubricating ability of powder lubricants for clean and high quality die casting. *J. Mater. Process. Technol.* 130, 289–293.

- Kubicek, P., Lesko, J., 1979. Determination of the kinetic-parameters from nonisothermal measurements with a general temperature program. *Thermochim. Acta* 31, 21-29.
- Lee, I.S., Nguyen, T.T., Leigh, G.M., 1989. Spray cooling of die casting dies. *Aust. Die Cast. Assoc.*, 53-69.
- Liu, G.W., Morsi, Y.S., Clayton, B.R., 2000. Characterization of the spray cooling heat transfer involved in a high pressure die casting process. *Int. J. Therm. Sci.* 39, 582-591.
- Mudawar, I., Estes, K.A., 1996. Optimizing and predicting CHF in spray cooling of a square surface. *J. Heat Transfer* 118, 672-679.
- Pautsch, A.G., Shedd, T.A., 2005. Spray impingement cooling with single- and multiple-nozzle arrays. Part I: Heat transfer data using FC-72. *Int. J. Heat Mass Transfer* 48, 3167-3175.
- Piskoti, C.R., 2003. New study turns up the heat on die spray cooling. *Die Cast. Eng.*, 44-45.
- Reichelt, L., Meingast, U., Renz, U., 2002. Calculating transient wall heat flux from measurements of surface temperature. *Int. J. Heat Mass Transfer* 45 (3), 579-584.
- Sabau, A.S., E.C. Hatfield, Measurement of heat flux and heat transfer coefficient due to spray application for the die casting process, *Proc. Inst. Mech. Eng., Part B, J. Eng. Manuf.*, Vol. 221, Issue B8, in press.
- Sabau, A.S., Wu, Z., 2007. Evaluation of a heat flux sensor for spray cooling for the die casting processes. *J. Mater. Process. Technol.* 182, 312-318.
- Stewart, I., Massingham, J.D., Hagers, J.J., 1995. Heat transfer coefficient effects on spray cooling. In: *The 1995 AISE Annual Convention and Iron & Steel Exposition*, Pittsburgh, Pennsylvania, September 27.